

## Original Article

**Cite this article:** Yoshida T, Tomida T, Urikura A, Aoyama Y, Hosokawa Y, Hanamura M, and Endo M. (2023) Uncertainty in organ delineation using low-dose computed tomography images with high-strength iterative reconstruction technique in radiotherapy for prostate cancer. *Journal of Radiotherapy in Practice*. **22**(e18), 1–7. doi: [10.1017/S1460396921000571](https://doi.org/10.1017/S1460396921000571)

Received: 12 July 2021

Revised: 8 September 2021

Accepted: 15 September 2021

### Author for correspondence:

Tsukasa Yoshida, Department of Diagnostic Radiology, Shizuoka Cancer Center, 1007 Shimonagakubo, Nagaizumi, Sunto, Shizuoka, 411-8777, Japan. Tel: +81-55-989-5222. Fax: +81-55-989-5783. E-mail: [ts.yoshida@scchr.jp](mailto:ts.yoshida@scchr.jp)

# Uncertainty in organ delineation using low-dose computed tomography images with high-strength iterative reconstruction technique in radiotherapy for prostate cancer

Tsukasa Yoshida<sup>1,2</sup>, Tetsuya Tomida<sup>3</sup>, Atsushi Urikura<sup>1</sup>, Yuki Aoyama<sup>3</sup>, Yoichiro Hosokawa<sup>4</sup>, Masahiro Hanamura<sup>3</sup> and Masahiro Endo<sup>1</sup>

<sup>1</sup>Department of Diagnostic Radiology, Shizuoka Cancer Center, 1007 Shimonagakubo, Nagaizumi, Sunto, Shizuoka, 411-8777, Japan; <sup>2</sup>Department of Radiation Science, Hirosaki University Graduate School of Health Sciences, 66-1 Hon-cho, Hirosaki 036-8564, Japan; <sup>3</sup>Radiation and Proton therapy Center, Shizuoka Cancer Center, 1007 Shimonagakubo, Nagaizumi, Sunto, Shizuoka, 411-8777, Japan and <sup>4</sup>Department of Radiological Life Sciences, Division of Medical Life Sciences, Hirosaki University, 66-1 Hon-cho, Hirosaki 036-8564, Japan

## Abstract

**Introduction** This study aimed to investigate the uncertainty in organ delineation of low-dose computed tomography (CT) images using a high-strength iterative reconstruction (IR) during radiotherapy planning for the treatment of prostate cancer.

**Methods** Two CT datasets were prepared with different dose levels by adjusting the reconstruction slice thickness. Two observers independently delineated the prostate, seminal vesicles, bladder and rectum on both images without referring to other modality images. The delineated organ volumes were compared between both images. Observer delineation variability was assessed using Dice similarity coefficient (DSC) and mean distance to agreement. **Results** No significant differences regarding the delineated organ volumes were observed between the low- and standard-dose images for all organs. Regarding inter-observer variability, the DSC was relatively high for both images, whereas mean distance to agreement was not significantly different between images ( $p > 0.05$  for all). Intra-observer variability for each observer showed high DSC ( $>0.8$  and  $>0.9$  for seminal vesicles and other organs, respectively) but no significant differences in the mean distance to agreement ( $p > 0.05$  for all).

**Conclusions** Our results indicate that low-dose CT images with high-strength IR would be available for organ delineation in the radiotherapy treatment planning for prostate cancer.

## Introduction

Computed tomography (CT) remains the gold standard modality for radiotherapy treatment planning. In patients with prostate cancer, accurate organ delineation is required for precise radiotherapy, such as that delivered using volumetric modulation arc therapy (VMAT) because the target is close to organs at risk (OARs). However, organ delineation in the pelvis using CT images alone is challenging because of the low-contrast resolution of CT imaging compared with that of magnetic resonance imaging (MRI). Previous studies showed a large inter-observer variability of organ delineation in the prostate and seminal vesicles using CT images alone.<sup>1,2</sup> To reduce variability in inter-observer delineation, high-dose volumetric CT is useful for prostate radiotherapy.<sup>3,4</sup> Conversely, there is a concern regarding the increased radiation exposure because high-quality CT images can only be obtained by escalating the radiation dose.

Davis et al. conducted a systematic review to assess the CT scan protocols for radiotherapy treatment planning used in previous reports.<sup>5</sup> The results showed that several studies focused on image quality and variations in CT values because these factors are extremely important in CT simulations for radiotherapy. However, radiation exposure among patients was not comprehensively assessed even though CT radiation dose optimisation is essential according to as low as reasonably achievable (ALARA) principles. In addition, some researchers have paid attention to imaging dose associated with the modern treatment techniques for prostate cancer.<sup>6,7</sup>

Iterative reconstruction (IR) techniques have contributed greatly to dose reduction in diagnostic CT examination. IR can reduce the radiation dose among patients while maintaining the image quality and mitigating the streak artefact.<sup>8–10</sup> The benefit of IR stems principally from the lower radiation dose required. Conversely, IR-specific artefacts, such as a plastic-like or blotchy image appearance associated with higher IR levels, cause degradation of the image quality in diagnostic CT.<sup>11–13</sup> Noid et al. evaluated the application of the IR technique in four-dimensional CT scan to manage respiratory motion in radiotherapy.<sup>14</sup> The results showed that a higher-strength

**Table 1.** Patient characteristics

Characteristic	Value
Age (years)	
Median (range)	70 (60–73)
Gleason score	
< 7	1
7	4
≥ 7	2
T stage	
T1	2
T2	4
T4	1
Serum PSA <sup>a</sup> (ng/ml)	
< 10	4
10–19	2
≥ 20	1
Risk	
Low	1
Intermediate	4
High	2

<sup>a</sup>PSA: prostate-specific antigen.

IR reduced the radiation dose without impairing image quality; however, organ delineation was not assessed.

To date, it remains unclear whether texture changes in CT images associated with the IR technique affect pelvic organ delineation. Therefore, this study aimed to investigate the uncertainty in organ delineation of low-dose CT images using a high-strength IR technique in radiotherapy planning for the treatment of prostate cancer.

## Materials and Methods

### Study design

This retrospective study was approved by the institutional review board of the Shizuoka Cancer Center, and the requirement for informed consent was waived. All methods were performed in accordance with the relevant guidelines and regulations. Seven patients with localised prostate cancer who underwent planning CT scans between 1 April and 31 May 2018 were included. All patients were histologically diagnosed with prostate adenocarcinoma. Patient characteristics are summarised in Table 1.

### CT data acquisition

CT was performed using an 80-row multidetector-row CT scanner (Aquilion PRIME, Canon Medical Systems, Tochigi, Japan). All patients underwent CT examination using an immobilising bag in the supine position 1 h after urine collection. Acquisition parameters were as follows: reconstruction thickness/increment of 2/2 mm, tube current determined using an automatic tube current modulation (standard deviation of CT value was set at 10), tube voltage of 120 kV, rotation time of 0.5 s, pixel size of 0.96 × 0.96 mm, detector configuration of 0.5 mm × 80 rows,

reconstruction kernel of the soft tissue (FC13) and IR adaptive iterative dose reduction 3D (AIDR3D Mild). The volume CT dose index (CTDI<sub>vol</sub>) on the scan console was also recorded. CT scans were performed in all patients under free breathing.

### AIDR3D and AIDR3D enhanced

AIDR3D is a hybrid IR technique in which image noise is reduced in both raw data and/or image domain. In particular, iteration process to the projection data is performed to decrease image noise and artefacts due to photon starvation in the raw data domain. After back projection or in the image space, the image filter is applied to the individual body region to decrease image noise and preserve edge structure. Moreover, utilisation of AIDR3D enhanced further reduces image noise in accordance with the noise power spectrum model. Four and three types of strength can be selected in AIDR3D (weak, mild, standard and strong) and AIDR3D enhanced (mild, standard and strong), respectively.

### Preparation of CT dataset

We retrospectively reconstructed two datasets for each patient: virtual low-dose image (low-dose image) and standard-dose image (std-dose image). A low-dose image is acquired using a thin reconstruction thickness instead of a low exposure dose because performing an additional CT scan even at a low-dose level is not ethically acceptable due to the additional exposure to ionising radiation. In general, image noise in CT is inversely proportional to the square root of the slice thickness. Low-dose image is equivalent to the data obtained from half- and quarter-dose images compared with std-dose image (Supplemental Figure S1). As shown in Figure 1, std-dose images were reconstructed at a 2.0 mm thickness and increment using a AIDR3D Mild. The dataset of low-dose images was prepared using the following two steps. First, low-dose images were reconstructed at a 0.5 mm thickness and increment using high IR level (AIDR3D enhanced strong). The IR strength was determined to be equivalent to the level of image noise (standard deviation of the CT value, as shown in Supplemental Figure S4 between the two datasets). Second, the dataset for low-dose images included images in every fourth slice with the same number of CT images in both datasets. In this study, the slice thickness settings were such that CTDI<sub>vol</sub> in low-dose images was a quarter of that in std-dose images.

### Organ delineation

The CT dataset was transferred to the MIM software (MIM Maestro, version 6.4.3, MIM Software Inc., Cleveland, OH, USA). Organ delineation was independently performed by two medical physicists with prior training in this procedure (T.T. with 11-year experience and Y.A. with 2-year experience). According to the consensus for organ delineation,<sup>15</sup> two observers independently delineated the prostate, seminal vesicles, bladder and rectum on the low- and std-dose images of each patient without referring to other modality images. The order of CT images for organ delineation was randomised for each observer to reduce recall bias. Organ delineation was repeated after 3 months to assess intra-observer variability in delineation.

### Data analysis

Data analysis was performed using the MIM software. The delineated organ volumes were measured on low- and std-dose images for each observer. Inter- and intra-observer variabilities

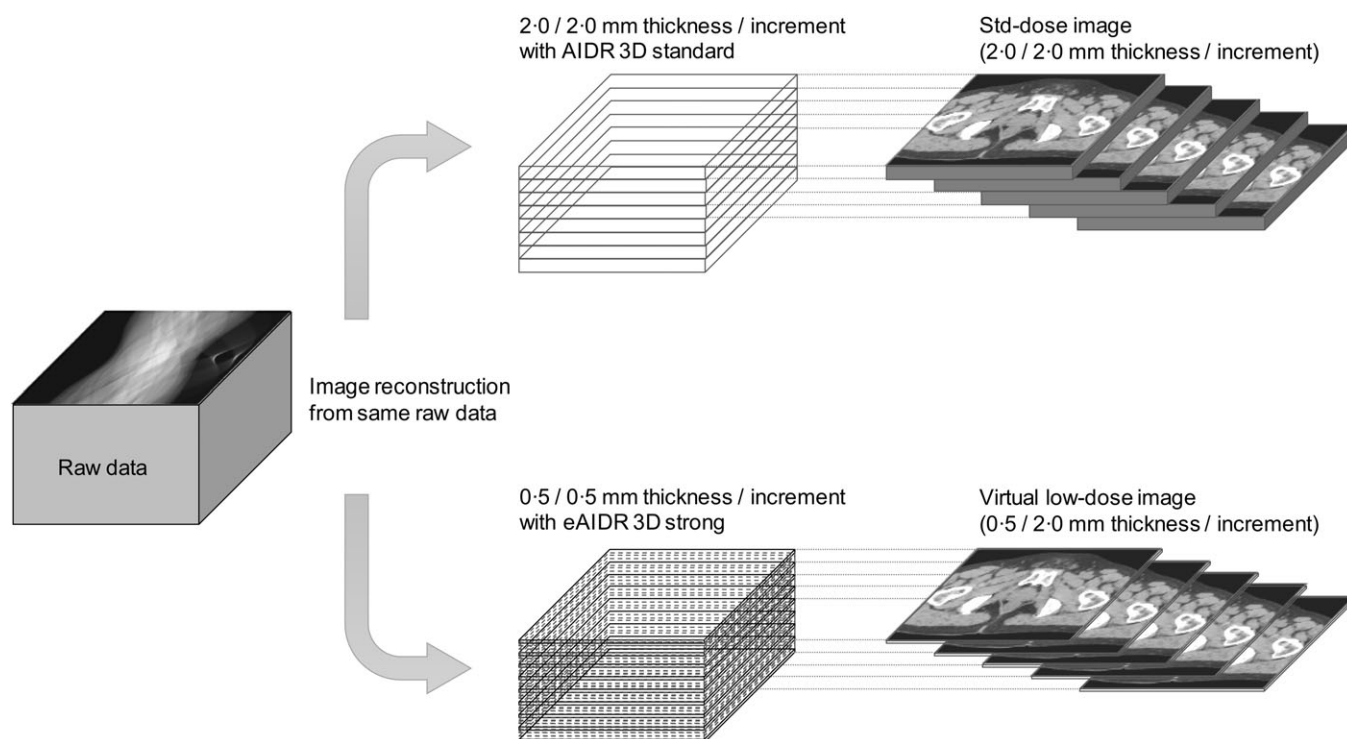


**Figure 1.** Preparation for computed tomography dataset.

Two different datasets were reconstructed from the same raw data. Standard-dose image (std-dose image) was reconstructed with 2.0/2.0-mm thickness/increment and applied using the adaptive iterative dose reduction 3D (ADR3D) standard. Virtual low-dose image was reconstructed by 0.5/0.5-mm thickness/increment and applied with ADR3D enhanced strength. Then, to obtain the same number of slices between datasets, the low-dose image was obtained every 2.0-mm increment (every four slice in dataset). The ADR3D strength was determined to have the same noise level between the two datasets.

were assessed using both the Dice similarity coefficient (DSC) and mean distance to agreement (MDA),<sup>16</sup> with the former indicating the spatial overlap between the structures and the latter indicating the mean values to measure the shortest distance from the surface of one delineation to that of another.  $DCS_{inter}$ ,  $DCS_{intra\_obs1}$  and  $DCS_{intra\_obs2}$  were defined as follows:

$$DSC_{inter} = \frac{2|X \cap Y|}{|X| + |Y|}$$

$$DSC_{intra\_obs1} = \frac{2|X_{1st} \cap X_{2nd}|}{|X_{1st}| + |X_{2nd}|}$$

$$DSC_{intra\_obs2} = \frac{2|Y_{1st} \cap Y_{2nd}|}{|Y_{1st}| + |Y_{2nd}|}$$

where X and Y are the respective delineations performed by observers 1 and 2, respectively.  $X_{1st}$  and  $X_{2nd}$  are the first and second delineations performed by observer 1, respectively.  $Y_{1st}$  and  $Y_{2nd}$  are the first and second delineations performed by observer 2, respectively.

### Statistical analysis

We compared the delineated organ volumes between the two datasets using a paired t-test. DSC and MDA were also compared using the Wilcoxon signed test and paired t-test, respectively. A  $p$ -value  $< 0.05$  was considered significant. Statistical analysis was performed using the R software version 3.2.3 (R Foundation for Statistical Computing, Austria; <http://www.R-project.org>).

### Results

The mean  $CTDI_{vol}$  were 5.6 (range 4.8–6.3) mGy on the low-dose images and 22.5 (range, 19.1–25.3) mGy on the std-dose images. Table 2 shows the delineated organ volumes between the low- and std-dose images. No significant differences in mean delineated organ volumes were observed between the images of each observer. Figure 2 shows the DSC for each image obtained between the observers. The median DSCs were  $> 0.9$  for the bladder and  $> 0.8$  for the other organs for both images. The median DSCs for low- and std-dose images were not significantly different ( $p > 0.05$  for all organs by both observers).

Table 3 shows respective MDAs obtained with low- and std-dose images between observers. No significant differences regarding the mean MDA were observed between the images ( $p > 0.05$  for all organs).

Figure 3 shows the DSCs for low- and std-dose images obtained from each organ. The median DSCs were  $> 0.8$  for the seminal vesicles and  $> 0.9$  for the other organs for both images. There were no significant differences in median DSCs between low- and std-dose images between observers ( $p > 0.05$  for all organs).

Table 4 shows the respective MDAs obtained with low- and std-dose images for each observer. No significant differences in mean MDA were observed between images for each observer ( $p > 0.05$  for all organs).

### Discussion

This is the first study to determine the delineated organ volumes as well as intra- and inter-observer variabilities in delineations using low-dose CT images with a high-strength IR technique for

**Table 2.** Delineated volume differences between low- and standard-dose images\*

	Volume (mL)							
	Observer 1				Observer 2			
	Low <sup>a</sup>	Standard	Diff	p-value <sup>b</sup>	Low	Standard	Diff	p-value
Prostate	26.25 ± 10.2	26.52 ± 11.34	0.27 (-1.31, 1.84)	0.69	29.32 ± 14.58	28.22 ± 12.22	1.10 (-2.54, 4.74)	0.49
Seminal vesicles	8.39 ± 4.44	8.60 ± 4.24	0.21 (-0.11, 0.54)	0.16	9.18 ± 5.0	9.71 ± 4.81	-0.53 (-1.24, 0.19)	0.12
Bladder	244.69 ± 112.9	241.66 ± 109.88	-3.03 (-8.27, 2.22)	0.21	236.81 ± 110.1	238.31 ± 109.39	-1.50 (-5.65, 2.66)	0.41
Rectum	44.84 ± 18.27	43.48 ± 16.09	-1.36 (-4.23, 1.54)	0.30	50.88 ± 20.02	49.36 ± 16.4	1.52 (-3.01, 6.05)	0.44

\*Data are presented as mean ± standard deviation.

<sup>a</sup>Low: Virtual low-dose image, Standard: standard-dose image. Diff indicates the mean of differences in delineated volumes between low- and standard-dose images; 95% confidence intervals are presented in parentheses.

<sup>b</sup>A p-value <0.05 was considered significant, as determined using paired t-test.

**Table 3.** Inter-Observer variability using MDA between low- and standard-dose images\*

	Mad <sup>a</sup> (mm)			
	Low	Standard	Diff <sup>b</sup>	p-value <sup>c</sup>
Prostate	1.70 ± 0.35	1.62 ± 0.31	0.085 (-0.36, 0.53)	0.66
Seminal vesicles	1.04 ± 0.08	1.21 ± 0.37	-0.17 (-0.51, 0.17)	0.27
Bladder	1.11 ± 0.18	1.33 ± 0.56	-0.22 (-0.77, 0.34)	0.38
Rectum	1.27 ± 0.35	1.29 ± 0.4	-0.017 (-0.31, 0.28)	0.89

\*Data are presented as mean ± standard deviation.

<sup>a</sup>dman: mean distance to agreement, Low: virtual low-dose image, Standard: standard-dose image.

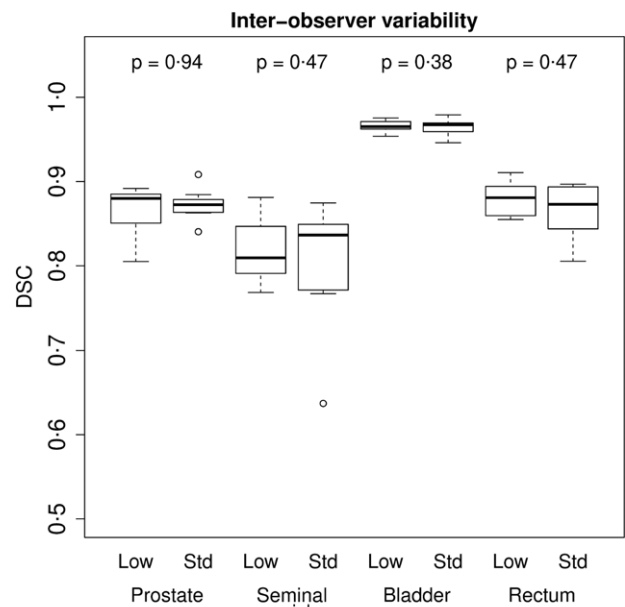
<sup>b</sup>Diff indicates mean differences of delineated volumes between low- and standard-dose images; 95% confidence intervals are presented in parentheses.

<sup>c</sup>An p-value <0.05 was considered significant, as determined using paired t-test.

radiotherapy treatment planning. Our results showed that the delineated organ volumes, DSCs and MDAs were not significantly different between the low- and std-dose images. While acquiring a treatment planning CT scan, dose constraints should not be strictly adapted for diagnostic imaging because accurate delineation of the target and OARs is required.<sup>17</sup> However, dose optimisation is still required from the perspective of patient exposure, even when acquiring a treatment planning CT scan. The IR technique can help manage both the image quality and dose reduction required for diagnostic purposes. Our findings suggest that the high-strength IR technique is effective for the treatment planning CT because it shows comparable delineation performance while reducing the radiation dose.

No significant difference in volume measurement was observed between the low- and std-dose images. McErlean et al. reported that small-sized lesions result in considerable variability in CT measurements.<sup>18</sup> Conversely, we found that the delineated seminal vesicle volumes showed a relatively good agreement between the two images. This result indicates that high-strength IR has a minor impact on the volume measurement.

The inter-observer variability in delineation assessed using DSC and MDA did not differ significantly between the two CT images. DSC was relatively high for all delineated organs, and our results are consistent with those reported in recent studies.<sup>19,20</sup>

**Figure 2.** Inter-observer variability in organ delineation.

Box-whisker plot shows the Dice similarity coefficient (DSC) between low- and standard-dose images for each organ.

The median DSC is relatively high (>0.8) and shows favourable agreement between images. No significant differences of DSC were observed between images (p = 0.94 for the prostate, p = 0.47 for the seminal vesicle, p = 0.38 for the bladder, and p = 0.47 for the rectum).

High-strength IR causes a peculiar artefact that changes the detailed structures on CT images.<sup>21</sup> However, no significant differences in inter-observer variation were observed between the two images. This is because the main source of delineation variability on the CT image between observers is the low-contrast resolution at tissue boundaries and not the slight texture differences.

Intra-observer variability also showed no significant differences between low- and std-dose images. Furthermore, the MDA and DSC values were similar or superior for intra-observer than inter-observer variability, as per our results. Previous studies have shown that intra-observer variability is comparable to inter-observer variability using CT images.<sup>18,22</sup> These results are in line with those of our study, indicating that high-strength IR may not increase the intra-observer variability of organ delineation.

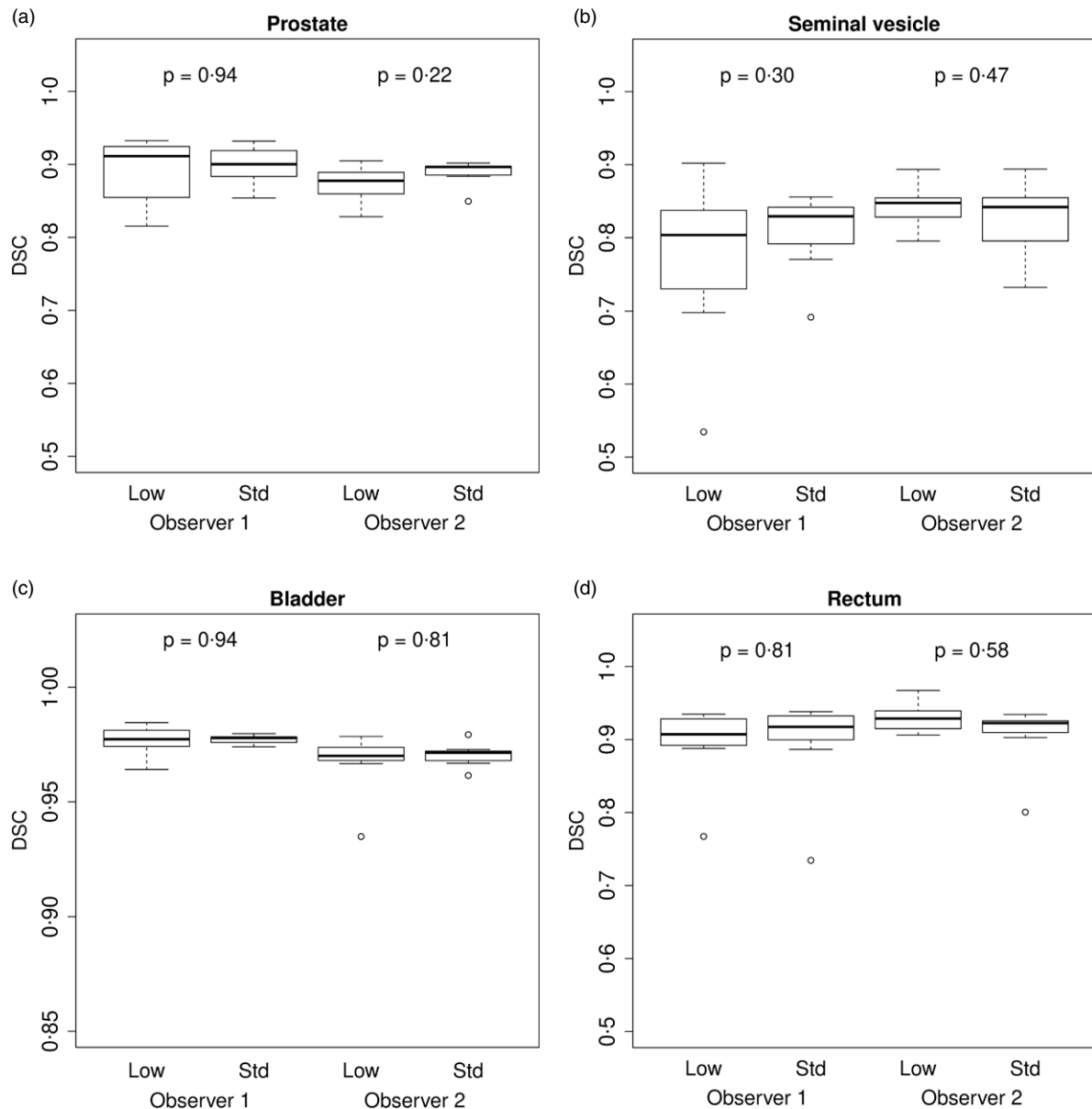


**Figure 3.** Intra-observer variability in organ delineation.

Box-whisker plot shows the Dice similarity coefficient (DSC) of the prostate (Figure 3a), seminal vesicle (Figure 3b), bladder (Figure 3c) and rectum (Figure 3d) between low- and std-dose images for each observer. DSC shows good agreement between images for each observer. The median DSC is not significantly different between images (prostate,  $p = 0.94$  for observer 1 and  $p = 0.22$  for observer 2; seminal vesicle,  $p = 0.30$  for observer 1 and  $p = 0.47$  for observer 2; bladder,  $p = 0.94$  for observer 1 and  $p = 0.81$  for observer 2; and rectum,  $p = 0.81$  for observer 1 and  $p = 0.58$  for observer 2).

Therefore, the image quality of low-dose CT will be sufficient to repeat the delineations available for the daily use of the treatment planning CT.

This study has several limitations. First, this was a retrospective study with a small sample size. Image noise was adjusted using slice thickness instead of low-dose protocols. High-strength IR with low-dose images deteriorates the quality of CT images. Moreover, the slice thickness of the two images was not similar, which may affect volume measurements because partial volume effect cannot be neglected for organ delineation especially in small organs such as seminal vesicle. Further studies in a larger sample should be conducted using a low-dose protocol with the same slice thickness. Second, the two observers were medical physicists, not radiation oncologists, physicians or radiologists; however, the results obtained

by our observers are comparable to those reported in a study by Roach et al., wherein the delineations were performed by multiple observers using the expert contours.<sup>20</sup> In addition, delineations performed by our observers were not compared with those from the simultaneous truth and performance level estimation (STAPLE) algorithm, which estimates ground-truth delineation.<sup>23</sup> Comparisons with delineations from multi-observer or STAPLE algorithms will provide more useful data on inter- and intra-observer variabilities in organ delineations. Finally, we did not include IR performed using equipment from different CT manufacturers. The image obtained using IR is not necessarily equivalent across vendors. The effects of IR technique on the delineation performance should be compared in a multi-vendor study in the future.

**Table 4.** Intra-Observer variability using MDA between low- and standard-dose images\*

	Mad <sup>a</sup> (mm)							
	Observer 1				Observer 2			
	Low	Standard	Diff	<i>p</i> -value <sup>b</sup>	Low	Standard	Diff	<i>p</i> -value
Prostate	1.37 ± 0.37	1.19 ± 0.17	-0.17 (-0.56, 0.22)	0.32	1.45 ± 0.35	1.53 ± 0.24	-0.081 (-0.53, 0.37)	0.67
Seminal vesicles	1.33 ± 0.68	1.05 ± 0.17	-0.28 (-0.95, 0.39)	0.35	1.02 ± 0.15	0.92 ± 0.21	0.099 (-0.19, 0.39)	0.43
Bladder	0.72 ± 0.13	0.72 ± 0.08	0.0027 (-0.17, 0.17)	0.97	1.11 ± 0.66	0.84 ± 0.05	0.28 (-0.35, 0.90)	0.32
Rectum	1.12 ± 0.69	1.13 ± 0.88	0.006 (-0.24, 0.25)	0.95	0.88 ± 0.23	0.80 ± 0.08	0.082 (-0.12, 0.29)	0.36

\*Data are presented as mean ± standard deviation.

<sup>a</sup>dman: mean distance to agreement, Low: virtual low-dose image, Standard: standard-dose image, Diff indicates the mean differences of MDA between low- and standard-dose images; 95% confidence intervals are presented in parentheses.

<sup>b</sup>A *p*-value < 0.05 was considered significant, as determined using paired *t*-test.

## Conclusion

Delineated volumes and observer variability in low-dose CT images with high-strength IR were investigated in this study. Delineation performance using low-dose images with the high-strength IR technique was comparable to that of std-dose images. Our results indicate that high-strength IR would be available for organ delineation in radiotherapy treatment planning for prostate cancer; however, larger-scale research is required.

**Supplementary Material.** To view supplementary material for this article, please visit <https://doi.org/10.1017/S1460396921000571>.

## Acknowledgements.

**Financial Support.** This study did not receive any specific grant from funding agencies in the public, commercial or not-for-profit sectors.

**Conflicts of Interest.** The authors declare that they have no conflicts of interest.

**Ethical Standards.** All procedures performed in studies involving human participants were in accordance with the ethical standards of the Institutional Review Board and with the 1964 Helsinki declaration and its later amendments or comparable ethical standards.

**Informed Consent.** For this type of study, formal consent is not required in our institution.

**Sources of Support.** None.

## References

- Villeirs GM, Van Vaerenbergh K, Vakaet L, et al. Interobserver delineation variation using CT versus combined CT + MRI in intensity-modulated radiotherapy for prostate cancer. *Strahlenther Onkol* 2005; 181 (7): 424–430. doi: [10.1007/s00066-005-1383-x](https://doi.org/10.1007/s00066-005-1383-x).
- Hentschel B, Oehler W, Strauss D, Ulrich A, Malich A. Definition of the CTV prostate in CT and MRI by using CT-MRI image fusion in IMRT planning for prostate cancer. *Strahlenther Onkol* 2011; 187 (3): 183–190. doi: [10.1007/s00066-010-2179-1](https://doi.org/10.1007/s00066-010-2179-1).
- Alasti H, Cho Y B, Catton C et al. Evaluation of high dose volumetric CT to reduce inter-observer delineation variability and PTV margins for prostate cancer radiotherapy. *Radiother Oncol* 2017; 125 (1): 118–123. doi: [10.1016/j.radonc.2017.08.012](https://doi.org/10.1016/j.radonc.2017.08.012). <https://www.ncbi.nlm.nih.gov/pubmed/28859933>.
- Cho Y B, Alasti H, Kong V et al. Impact of high dose volumetric CT on PTV margin reduction in VMAT prostate radiotherapy. *Phys Med Biol* 2019; 64 (6): 065017. doi: [10.1088/1361-6560/ab050f](https://doi.org/10.1088/1361-6560/ab050f). <https://pubmed.ncbi.nlm.nih.gov/30731450>
- Davis A T, Palmer A L, Nisbet A. Can CT scan protocols used for radiotherapy treatment planning be adjusted to optimize image quality and

- patient dose? A systematic review. *Br J Radiol* 2017; 90 (1076): 20160406. doi: [10.1259/bjr.20160406](https://doi.org/10.1259/bjr.20160406). <https://pubmed.ncbi.nlm.nih.gov/28452568>
- Chen GP, Noid G, Tai A, et al. Improving CT quality with optimized image parameters for radiation treatment planning and delivery guidance. *Phys Imaging Radiat Oncol* 2017; 4: 6–11. doi: [10.1016/j.phro.2017.10.003](https://doi.org/10.1016/j.phro.2017.10.003).
- Bell K, Heitfeld M, Licht N et al. Influence of daily imaging on plan quality and normal tissue toxicity for prostate cancer radiotherapy. *Radiat Oncol* 2017; 12 (1): 1–11. doi: [10.1186/s13014-016-0757-9](https://doi.org/10.1186/s13014-016-0757-9). <https://pubmed.ncbi.nlm.nih.gov/28069053/>
- Higaki T, Nakamura Y, Fukumoto W, Honda Y, Tatsugami F, Awai K. Clinical application of radiation dose reduction at abdominal CT. *Eur J Radiol* 2019; 111: 68–75. doi: [10.1016/j.ejrad.2018.12.018](https://doi.org/10.1016/j.ejrad.2018.12.018). <https://www.ncbi.nlm.nih.gov/pubmed/30691668>.
- Padole A, Ali Khawaja R D, Kalra M K, Singh S. CT radiation dose and iterative reconstruction techniques. *AJR Am J Roentgenol* 2015; 204 (4): W384–W392. doi: [10.2214/AJR.14.13241](https://doi.org/10.2214/AJR.14.13241). <https://www.ncbi.nlm.nih.gov/pubmed/25794087>.
- Ishikawa Y, Urakura A, Yoshida T, Takiguchi K, Nakaya Y. Radiation dose optimization for the bolus tracking technique in abdominal computed tomography: usefulness of real-time iterative reconstruction for monitoring scan. *Radiol Phys Technol* 2017; 10 (2): 155–160. doi: [10.1007/s12194-016-0378-x](https://doi.org/10.1007/s12194-016-0378-x). <https://www.ncbi.nlm.nih.gov/pubmed/27696286>.
- Schindera S T, Odedra D, Raza S A et al. Iterative reconstruction algorithm for CT: can radiation dose be decreased while low-contrast detectability is preserved? *Radiology* 2013; 269 (2): 511–518. doi: [10.1148/radiol.13122349](https://doi.org/10.1148/radiol.13122349). <https://www.ncbi.nlm.nih.gov/pubmed/23788715>.
- Urukura A, Hara T, Ichikawa K et al. Objective assessment of low-contrast computed tomography images with iterative reconstruction. *Phys Med* 2016; 32 (8): 992–998. doi: [10.1016/j.ejmp.2016.07.003](https://doi.org/10.1016/j.ejmp.2016.07.003). <https://www.ncbi.nlm.nih.gov/pubmed/27422374>.
- Morsbach F, Desbiolles L, Raupach R, Leschka S, Schmidt B, Alkadhi H. Noise texture deviation: a measure for quantifying artifacts in computed tomography images with iterative reconstructions. *Invest Radiol* 2017; 52 (2): 87–94. doi: [10.1097/RLI.0000000000000312](https://doi.org/10.1097/RLI.0000000000000312). <https://www.ncbi.nlm.nih.gov/pubmed/27548343>.
- Noid G, Tai A, Chen G P, Robbins J, Li X A. Reducing radiation dose and enhancing imaging quality of 4DCT for radiation therapy using iterative reconstruction algorithms. *Adv Radiat Oncol* 2017; 2 (3): 515–521. doi: [10.1016/j.adro.2017.04.003](https://doi.org/10.1016/j.adro.2017.04.003). <https://pubmed.ncbi.nlm.nih.gov/29114620>.
- Salembier C, Villeirs G, De Bari B et al. ESTRO ACROP consensus guideline on CT- and MRI-based target volume delineation for primary radiation therapy of localized prostate cancer. *Radiother Oncol* 2018; 127 (1): 49–61. doi: [10.1016/j.radonc.2018.01.014](https://doi.org/10.1016/j.radonc.2018.01.014). <https://www.ncbi.nlm.nih.gov/pubmed/29496279>.
- Jena R, Kirkby N F, Burton K E, Hoole A C, Tan L T, Burnet N G. A novel algorithm for the morphometric assessment of radiotherapy treatment planning volumes. *Br J Radiol* 2010; 83 (985): 44–51. doi: [10.1259/bjr/27674581](https://doi.org/10.1259/bjr/27674581). <https://www.ncbi.nlm.nih.gov/pubmed/19620177>.

17. Li H, Yu L, Anastasio M A et al. Automatic CT simulation optimization for radiation therapy: A general strategy. *Med Phys* 2014; 41 (3): 031913. doi: [10.1118/1.4866377](https://doi.org/10.1118/1.4866377). <https://www.ncbi.nlm.nih.gov/pubmed/24593731>.
18. McErlean A, Panicek D M, Zabor E C et al. Intra- and interobserver variability in CT measurements in oncology. *Radiology* 2013; 269 (2): 451–459. doi: [10.1148/radiol.13122665](https://doi.org/10.1148/radiol.13122665). <https://www.ncbi.nlm.nih.gov/pubmed/23824993>.
19. Shahedi M, Halicek M, Guo R, Zhang G, Schuster D M, Fei B. A semiautomatic segmentation method for prostate in CT images using local texture classification and statistical shape modeling. *Med Phys* 2018; 45 (6): 2527–2541. doi: [10.1002/mp.12898](https://doi.org/10.1002/mp.12898). <https://www.ncbi.nlm.nih.gov/pubmed/29611216>.
20. Roach D, Holloway L C, Jameson M G et al. Multi-observer contouring of male pelvic anatomy: highly variable agreement across conventional and emerging structures of interest. *J Med Imaging Radiat Oncol* 2019; 63 (2): 264–271. doi: [10.1111/1754-9485.12844](https://doi.org/10.1111/1754-9485.12844). <https://www.ncbi.nlm.nih.gov/pubmed/30609205>.
21. Kataria B, Nilsson Althén J, Smedby Ö, Persson A, Sökjer H, Sandborg M. Assessment of image quality in abdominal computed tomography: effect of model-based iterative reconstruction, multi-planar reconstruction and slice thickness on potential dose reduction. *Eur J Radiol* 2020; 122: 108703. doi: [10.1016/j.ejrad.2019.108703](https://doi.org/10.1016/j.ejrad.2019.108703).
22. Choi H J, Kim Y S, Lee S H et al. Inter- and intra-observer variability in contouring of the prostate gland on planning computed tomography and cone beam computed tomography. *Acta Oncol* 2011; 50 (4): 539–546. doi: [10.3109/0284186X.2011.562916](https://doi.org/10.3109/0284186X.2011.562916). <https://www.ncbi.nlm.nih.gov/pubmed/21391773>.
23. Warfield S K, Zou K H, Wells W M. Simultaneous truth and performance level estimation (STAPLE): an algorithm for the validation of image segmentation. *IEEE Trans Med Imaging* 2004; 23 (7): 903–921. doi: [10.1109/TMI.2004.828354](https://doi.org/10.1109/TMI.2004.828354). <https://www.ncbi.nlm.nih.gov/pubmed/15250643>.